Hydrodynamics of Falling Mine in Water Column

Peter C. Chu, Anthony F. Gilles, Chenwu Fan, Peter Fleischer

Abstract-- **The hydrodynamic features of a falling mine into the water column is investigated experimentally. The experiment consisted of dropping three cylindrical model mines of various lengths into a pool where the trajectories were filmed from two angles. The controlled parameters were, mine parameters (length to diameter ratio, center of mass location), and initial conditions (initial velocity, and drop angle). Results indicate that center of mass position has the largest influence on the mines' trajectory and that accurate trajectory modeling requires the inclusion of both momentum and moment equations. A statistical-dynamic model has been established to predict the trajectories of the falling mines.**

Key Words— **Mine impact burial, momentum of mine, moment of momentum of mine, mine impact burial prediction model, mine drop experiment (MIDEX).**

1. INTRODUCTION

ON December 31, 1991 the Union of Soviet Socialist Republics (USSR) effectively ceased to exist under international law and the Cold War ended (Fischer 1999). In response, the Navy-Marine Corps team developed a new strategic concept, "From the Sea" (FTS), which provides a framework for Naval operations into the 21st century. FTS effectively shifted operational focus from blue water operations to sea-based power projection into regional littoral areas. FTS, the 1994 revision "Forward From the Sea" (FFTS) and "Operational Maneuver from the Sea" (OMFTS) all provide guiding principles for sea-based power projection to regional littoral areas of the world.

One of the greatest threats to U.S. sea-based power projection in littoral areas is the naval mine. Mines were first developed in 1776 and have been used in most major conflicts since. Today, an estimated 50 countries possess some sort of mining capability. (Lehr 2000) Mines can be used in both offensive and defensive roles. Offensively, they can be placed in enemy waters or nearby sea-lanes in order to harass military and commercial shipping. Defensively, they can be used to delay or prevent amphibious assaults or to deny command of the sea. The Wonsan Korea Mine Crisis and Iraq's use of mines during Desert Storm provide excellent examples of the value of the naval mine as a defensive weapon. Shortly after the October 1950 Wonsan, Korea mine crisis, then Chief of Naval Operations Admiral Forest Sherman exclaimed, ``when you can't go where you want to, when you want to, you haven't got command of the sea. Command of the sea is the bedrock for all of our war plans. We have always been submarine-conscious and air-conscious. We have now commenced to become mine-conscious beginning last week." (Boorda 1999).

Within the past 15 years three U.S. ships, the USS Samuel B. Roberts (FFG-58), Tripoli (LPH-10) and Princeton (CG-59) have fallen victim to mines. Total ship damages were $125 million while the mines cost approximately $30 thousand. (Boorda 1999) Mines have evolved over the years from the dumb ``horned" contact mines that damaged the Tripoli and Roberts to ones that are relatively sophisticated - non-magnetic materials, irregular shapes, anechoic coatings, multiple sensors and ship count routines. Despite their increased sophistication, mines remain inexpensive and are relatively easy to manufacture, upkeep and place. As such, they are an efficient, yet potent, force multiplier and are widely available to any country or group who has a modest ability to purchase them.

Naval mines are characterized by three factors: position in water (bottom, moored, rising, floating), method of delivery (aircraft, surface, subsurface) and method of actuation (acoustic and/or magnetic influence, pressure, contact, controlled). The littoral battlespace is divided into five regions based upon water depth. Within each of these regions naval forces can encounter multiple types of threats (Fig. 1). The littoral regions are:

- Deep Water (DW). Water depths: > 300 ft. Threat: mainly moored and rising mines, although a few large bottom mines exist.
- Shallow Water (SW). Water depths: from 40 to 300 ft. Threat: bottom, moored and rising.
- Very Shallow Water (VSW). Water depths: from 10 to 40 ft. Threat: bottom, moored, rising and controlled.
- Surf Zone (SZ). Water depths: < 10 ft. to the beach itself. Threat: same as VSW but land mines and obstacles can also be encountered.
- Craft Landing Zone (CLZ). Water depths: the beach itself. Threat: conventional land mines and obstacles. (U.S. Naval Mine Warfare Plan 2000)

The shift in focus from the blue water to the littoral has brought many new challenges to the warfighter. The greatest is what impact will the highly variable littoral environment have on future operations, particularly mine countermeasures (MCM). The most influential environmental parameter to successful MCM operations is the local bathymetry character of the bottom. This key

Manuscript received January 15, 2002. This work was supported by the U.S. Office of Naval Research, Naval Oceanographic Office, and Naval Postgraduate School.

Peter C. Chu and Chenwu Fan are with the Naval Postgraduate School, Monterey, CA 93943 USA (telephone: 831-677-3688, e-mail: chu@nps.navy.mil, fan@nps.navy.mil).

A.F. Gilles, is with Naval Oceanographic Office, Stennis Space Center, MS 39529 USA (e-mail: gillesa@navo.navy.mil).

P. Fleischer is with the Naval Oceanographic Office, Stennis Space Center, MS 39529 USA (e-mail: fleischerp@navo.navy.mil).

parameter often determines whether an area should be swept or hunted. Bottom clutter in the form of rock outcrops, coral reefs, man-made debris and irregularities in slope provide false contacts or create shadow zones that increase overall clearance times. Soft bottom sediments such as marine clays and silts cause a high degree of mine burial upon impact. These buried or partially buried bottom mines are of greatest concern to the MCM planner.

Environmental data collection in a potential adversaries' littoral region is often hampered by inaccessibility. This lack of accurate data causes a certain degree of uncertainty in MCM planning. As a result, several numerical models for predicting mine impact burial (IB) have been developed. The most promising IB model was originally developed by Arnone and Bowen in 1980. Later improvements by Satkowiak (1987), Hurst (1992), Chu et al. (1998, 2000a, b) and others have resulted in the current version, IMPACT 25. IMPACT 25 creates a two-dimensional time history of a cylindrical mine as it falls through air, water and sediment phases. IB prediction is largely calculated from the marine sediment characteristics and mine impact orientation and velocity. Chu et al. (2001) found overprediction of burial depth by IMPACT25 after analyzing the synchronized environmental and mine burial data collected during the Mine Impact Burial Prediction Experiment (MIBEX) in the Monterey Bay in June 2000.

The essential elements of the mine impact burial model translate into the science and engineering of hydrodynamic process of a falling object and of sediment transport. Any solid object falling through fluid (air and water) should obey two physical principles: (a) momentum balance, and (b) moment balance. The current IMPACT25 model only considers the momentum balance of the mine and disregards the moment balance of the mine. Such an incomplete hydrodynamics in the model leads to unrealistic prediction of the mine falling in the water (no helicoidal motion). If considering momentum and moment balance, the falling object should have a helicoidal motion. Without the helicoidal motion, the IMPACT25 may over-predict the impact burial depth.

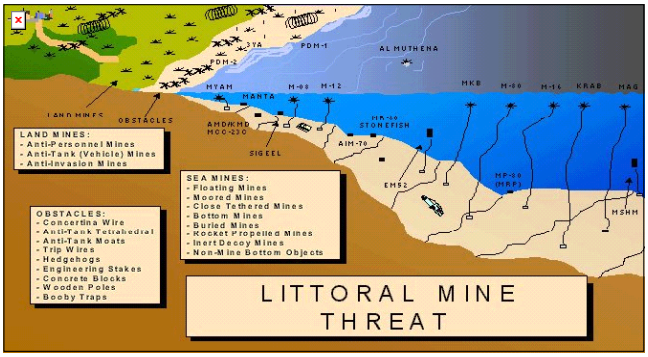

Figure1. Littoral mine threat (from Rhodes, 1998).

In this study, a nonlinear dynamical system is established for the movement of a nonuniform (center of gravity not the same as the center of volume) cylindrical model mine in the water column. A mine-drop experiment was conducted. The experimental results show the nonlinear characteristics of the trajectory pattern. The data collected from the experiment can be used for mine impact burial prediction model development and verification.

2. DYNAMICS

A. Earth Coordinate System

Two coordinate systems are used to describe a mine falling through the water column: earth and relative coordinates. The earth coordinate system is fixed to the Earth surface with horizontal sides as x and y-axes (along the two sides of the pool), and vertical direction as z-axis (upward positive, Fig. 2). Suppose a mine falling into the water column. The mine rotates around its main axis (r_1) with an angle ψ_1 and an angular velocity of Ω. Its position is represented by the center of mass (COM), and its orientation is represented by two angles: ψ_2 and ψ_3 (Fig. 3). Here, ψ_2 is the angle between the r_1-axis and the horizontal plane; and ψ_3 is the angle between the projection of the main axis in the (x, y) plane and the x-axis. The angle, $\psi_2 + \pi/2$, is usually called attitude.

The relative coordinate is rigidly connected with the mine. The origin (O) of the relative coordinate system coincides with the center of mass (COM); the r_1-axis is along the central line of the mine; the r_2-axis is perpendicular to the plane constructed by r_1-axis and z-axis (r_1-z plane); and the r_3-axis lies in the (r_1-z) plane and is perpendicular to r_1-axis. The selection of axes (x, y, z) and (r_1, r_2, r_3) follows the right-hand rule. Let $\mathbf{V}^* = (V_1^*, V_2^*, V_3^*)$ be the three components of the velocity of COM, i.e., be the origin velocity of the coordinate system (r_1, r_2, r_3). The geometric center (GC) is located at (χ, 0, 0). For GC below COM, $\chi > 0$, and for GC above COM, $\chi < 0$. The relative coordinate system (r_1, r_2, r_3) is obtained through the translation and two rotations ψ_2 and ψ_3 of the earth coordinate system. Let the position vector $\mathbf{P}$ be represented by $\mathbf{P_E}$ and $\mathbf{P_B}$ in the earth and relative coordinate systems, $\mathbf{P_E}$ and $\mathbf{P_B}$ are connected by

$$\mathbf{P_E} = \begin{bmatrix} \cos\psi_3 & -\sin\psi_3 & 0 \\ \sin\psi_3 & \cos\psi_3 & 0 \\ 0 & 0 & 1 \end{bmatrix} \begin{bmatrix} \cos\psi_2 & 0 & \sin\psi_2 \\ 0 & 1 & 0 \\ -\sin\psi_2 & 0 & \cos\psi_2 \end{bmatrix} \mathbf{P_B} + \begin{bmatrix} x_m^* \\ y_m^* \\ z_m^* \end{bmatrix} \quad (1)$$

where (x_m*, y_m*, z_m*) represent the position of COM in the earth coordinate system.

B. Nonlinear Dynamical Equations

Any solid object falling through a fluid (air and water) should obey two physical principles: (1) momentum balance and (2) moment of momentum balance. Let $\mathbf{V}_w = (V_{w1}, V_{w2}, V_{w3})$ be the water velocity, and $(\omega_1^*, \omega_2^*, \omega_3^*)$ be the components of the angular velocity, referring to the direction of the relative coordinate system. The independent and dependent variables are made non-dimensional by:

$$t = \sqrt{\frac{g}{L}}t^*, \quad \omega = \sqrt{\frac{L}{g}}\omega^*, \quad \mathbf{V} = \frac{\mathbf{V}^*}{\sqrt{gL}},$$

where g is the gravitational acceleration, and L the length of the mine. The non-dimensional momentum equations for COM are given by (Mises 1959)

$$\frac{dV_1}{dt} + \omega_2 V_3 - \omega_3 V_2 = \frac{\rho - \rho_w}{\rho}\sin\psi_2 + \frac{F_1^*}{\rho g \Pi}, \tag{2a}$$

$$\frac{dV_2}{dt} + \omega_3 V_1 = \frac{F_2^*}{\rho g \Pi}, \tag{2b}$$

$$\frac{dV_3}{dt} - \omega_2 V_1 = -\frac{\rho - \rho_w}{\rho}\cos\psi_2 + \frac{F_3^*}{\rho g \Pi}, \tag{2c}$$

where Π is the volume of the mine, ρ the mine density, ρ_w the water density, (F_1*, F_2*, F_3*) the components of water drag. The non-dimensional equations of the moment of momentum for axial symmetric mine are

$$\frac{d\Omega}{dt} + \frac{J_3 - J_2}{J_1}\omega_2\omega_3 = \frac{LM_1^*}{gJ_1}, \tag{3a}$$

$$\frac{d\omega_2}{dt} = -\frac{\chi^* \Pi(\rho - \rho_w)L}{J_2}\cos\psi_2 + \frac{LM_2^*}{gJ_2}, \tag{3b}$$

$$\frac{d\omega_3}{dt} = \frac{LM_3^*}{gJ_3}, \tag{3c}$$

where χ^* is the distance between COM and geometric center (GC), (M_1*, M_2*, M_3*) the components of the moment due to water drag, (J_1, J_2, J_3) the three moments of gyration,

$$J_1 = \int (r_2^2 + r_3^2)dm^*, \quad J_2 = \int (r_3^2 + r_1^2)dm^*,$$

$$J_3 = \int (r_1^2 + r_2^2)dm^* . \tag{4}$$

The orientation of the mine (ψ_2, ψ_3) is determined by

$$\frac{d\psi_2}{dt} = \omega_2, \qquad \cos\psi_2 \frac{d\psi_3}{dt} = \omega_3. \tag{5}$$

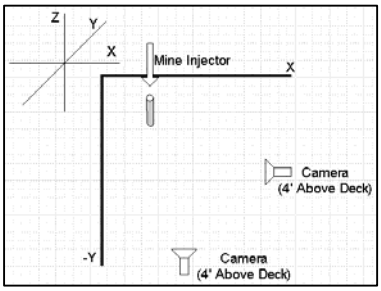

Figure 2. Earth coordinate system.

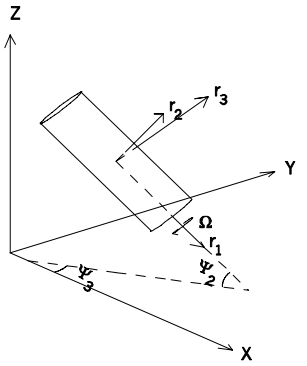

Figure 3. Cylinder orientation and relative coordinate system.

The eight non-dimensional nonlinear equations (2a-c), (3a-c), and (5) are the basic system for determining the mine movement in the water column.

3. MODEL MINES

A. Description

Three model mines were used for the drop experiment at the Naval Postgraduate School swimming pool. All had a circular diameter of 4 cm, however the lengths were 15, 12 and 9 cm respectively. The bodies were constructed of rigid plastic with aluminum-capped ends. Inside each was a threaded bolt, running lengthwise across the mine, and an internal weight (Fig. 4). The internal cylindrical weight made by copper was used to vary the mine's center of mass and could be adjusted fore or aft. The center of gravity of the model mine is the origin of the body fixed coordinate system.

The model mine is composed of six uniform cylindrical parts (Fig. 4): (a) a plastic hollow cylinder $C^{(1)}$ with mass of m_1, outer and inner radii of R_1 and R_2, length of (L -2l_1), and the center of gravity for the part (COMP) to be at its geometric center located along the r_1-axis at $r_1 = \chi$; (b) an aluminum-capped left end (Fig. 5) solid cylinder $C^{(2)}$ with mass of m_2, radius of R_1, length of l_1, and COMP located along the r_1-axis at $r_1 = L/2 - l_1/2 + \chi$; (c) an aluminum-capped right end solid cylinder $C^{(3)}$ with mass of m_3, radius of R_1, length of l_1, and COMP located along the r_1-axis at $r_1 = L/2 - l_1/2 - \chi$; (d) a cylindrical thread $C^{(4)}$ with mass of m_4,

radius of R_3, length of (L - $2l_1$), and COMP located along the r_1-axis at $r_1 = \chi$; (e) a cylindrical threaded bolt $C^{(5)}$ with mass of m_5, out and inner radii of R_2 and R_3, length of l_2, and COMP located along the r_1-axis at $r_1 = L/2 - \chi - l_1 - l_2/2$; (f) an adjustable copper cylindrical weight $C^{(6)}$ with mass of m6, outer and inner radii of R_2 and R_3, length of l_3, and COMP located along the r_1-axis at r1 = $\delta + \chi$, where δ is the distance between the COMP of the adjustable weight and the geometric center of the model mine.

B. Moments of Gyration

Since the six parts (all mines) all have uniform mass distribution, the moments of gyration for these parts are:

$$J_1^{(1)} = \frac{m_1}{2}(R_1^2 + R_2^2),\quad J_1^{(2)} = \frac{m_2}{2}R_1^2,\quad J_1^{(3)} = \frac{m_3}{2}R_1^2,$$

$$J_1^{(4)} = \frac{m_4}{2}R_3^2,\quad J_1^{(4)} = \frac{m_4}{2}R_3^2,\quad J_1^{(6)} = \frac{m_6}{2}(R_2^2 + R_3^2),$$

$$J_2^{(1)} = J_3^{(1)} = \frac{m_1}{12}\left[3R_1^2 + 3R_2^2 + (L-2l_1)^2\right],$$

$$J_2^{(2)} = J_3^{(2)} = \frac{m_2}{12}(3R_1^2 + l_1^2),\qquad J_2^{(3)} = J_3^{(3)} = \frac{m_3}{12}(3R_1^2 + l_1^2),$$

$$J_2^{(4)} = J_3^{(4)} = \frac{m_4}{12}\left[3R_3^2 + (L-2l_1)^2\right],$$

$$J_2^{(5)} = J_3^{(5)} = \frac{m_5}{12}(3R_2^2 + 3R_3^2 + l_2^2),$$

$$J_2^{(6)} = J_3^{(6)} = \frac{m_6}{12}(3R_2^2 + 3R_3^2 + l_3^2), \qquad (6)$$

where the superscripts for the moments indicate the cylindrical parts. The resultant moments of gyration is computed by

$$J_1 = \sum_{j=1}^{6} J_1^{(j)},$$

$$J_2 = J_3 = \sum_{j=1}^{6} J_2^{(j)} + m_1\chi^2 + m_2\left(\frac{L-l_1}{2} - \chi\right)^2 + m_3\left(\frac{L-l_1}{2} + \chi\right)^2$$

$$+ m_4\chi^2 + m_5\left(\frac{L}{2} - \chi - l_1 - \frac{l_2}{2}\right)^2 + m_6(\delta + \chi)^2. \qquad (7)$$

According to the definition of COM, the coordinate of GC (χ) is determined by

$$\chi = \frac{\left[m_5(L/2 - l_1 - l_2/2) - m_6\delta\right]}{\sum_{j=1}^{6} m_j}, \qquad (8)$$

which indicates how the adjustable weight determines the location of COM for the model mine.

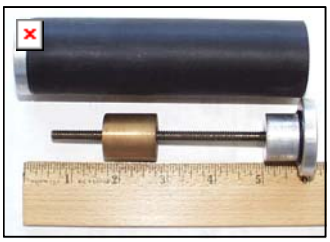

Figure 4. Internal components of the model mine.

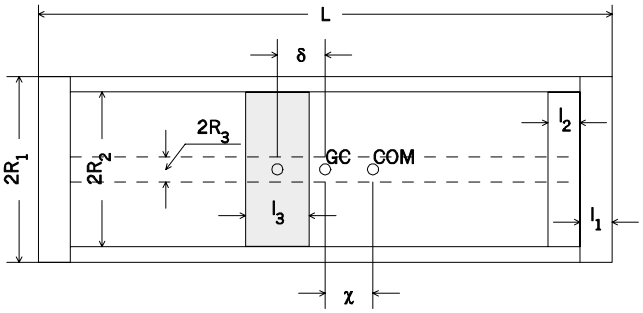

Figure 5. Internal structure of the model mine.

C. Model Parameters

C.1. Length/Diameter and Density Ratios

Our goal was to choose a scale that was somewhat representative of the real world ratio of water depth to mine length, but at the same time would be large enough to film and would not damage the pool's bottom. The model mines were based on the realistic assumption that a 3 m mine is laid in water depths of 45 m, thus producing a 15:1 ratio. The depth of the pool is 2.4 m. From this ratio, the length (L) of the model mine is chosen as 15 cm. The addition of a 12 and 9 cm length allowed for later comparison of the sensitivity of water phase trajectory to the ratio of mine length over diameter. The outer radius of the model mine is 2 cm. The length/diameter ratios (L/D) are 15/4, 12/4, and 9/4. The corresponding density ratios (ρ/ρ_w) are 1.70, 1.68, and 1.88, respectively.

C2. χ-Value

In each of the three model mines, the location of the weight (i,e., the value of δ) is adjustable. Use of (7) location of the COM (χ-value) can be determined (Table 1). The positive χ-value indicates that COM is below the geometric center, and the negative χ-value indicates that COM is above the geometric center.

Table 1. Model L/D, density ratio, and χ-value (unit: cm).

Mine	L/D	ρ / ρ_w	χ_1	χ_2	χ_0	χ_{-1}	χ_{-2}
1	15/4	1.70	1.85	3.69	0	-1.85	-3.69
2	12/4	1.68	1.21	2.43	0	-1.21	-2.43
3	9/4	1.88	0.68	1.37	0	-0.68	-1.37

4. MINE DROP EXPERIMENT

An mine drop experiment (MIDEX) was conducted at the NPS swim pool in June 2001. The purpose of the experiment is to collect data about mine's motion in the water column for various combinations of the model mine parameters. It basically consisted of dropping each of three model mines into the water where each drop was recorded underwater from two viewpoints. Figure 6 depicts the overall setup. The controlled parameters for each drop were: *L*/D ratio, χ-value, initial velocity (V_{in}), and drop angle. The Earth's coordinate system is chosen with the origin at the corner of the swimming pool with the two sides as *x*- and *y*-axes and the vertical *z*-axis. The initial injection of mine was in the (*y*, *z*) plane (Fig. 2).

A. Initial Velocity

Initial velocity (V_{in}) was calculated by using the voltage return of an infrared photo detector located at the base of the mine injector. The infrared sensor produced a square wave pulse when no light was detected due to blockage caused by the mine's passage. The length of the square wave pulse was converted into time by using a universal counter. Dividing the mine's length by the universal counter's time yielded V_{in}. The mines were dropped from several positions within the injector mechanism in order to produce a range of V_{in}. The method used to determine V_{in} required that the infrared light sensor be located above the water's surface. This distance was held fixed throughout the experiment at 10 cm.

B. Drop Angle

The drop angle (initial $\psi_2^{(in)}$) was controlled using the drop angle device. Five screw positions marked the 15°, 30°, 45°, 60°, and 75°. The drop angles were determined from the lay of the pool walkway, which was assumed to be parallel to the water's surface. A range of drop angles was chosen to represent the various entry angles that air and surface laid mines exhibit. This range produced velocities whose horizontal and vertical components varied in magnitude. This allowed for comparison of mine trajectory sensitivity with the varying velocity components.

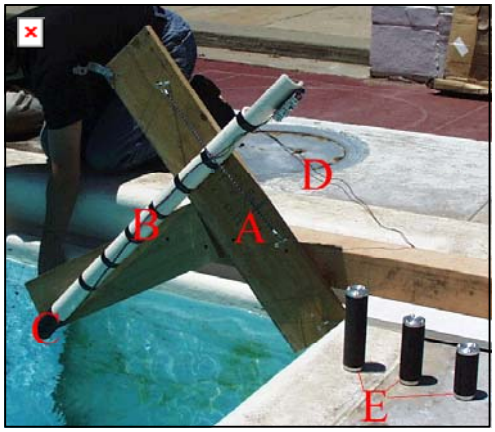

Figure 6. MIDEX equipment.

C. Methodology

For each run the mines were set to a χ-value. For positive χ-value, the mines were placed into the injector so that the COM was located below the geometric center. For negative χ-value, the COM was located above the geometric center to release. A series of drops were then conducted in order of decreasing mine length for each angle. Table 2 indicates number of drops conducted for different drop angles and χ-value for *L*/*D* = 15/4. Number of drops for other *L*/*D* ratios (12/4, 9/4) is comparable to that for *L*/*D* ratio of 15/4. All together there were 712 drops. Each video camera had a film time of approximately one hour. At the end of the day, the tapes were replayed in order to determine clarity and optimum camera position.

Table 2. Number of drops conducted for different drop angles and χ-values for L/D = 15/4.

$\psi_2^{(in)}$	15°	30°	45°	60°	75°
χ_2	13	15	15	15	12
χ_1	9	15	15	15	9
χ_0	12	14	15	18	6
χ_{-1}	0	6	6	6	0
χ_{-2}	2	6	6	0	0

5. DATA RETRIEVAL AND ANALYSIS

A. Data Retrieval

Upon completion of the drop phase, the video from each camera was converted to digital format. The digital video for each view was then analyzed frame by frame (30 Hz) in order to determine the mine's position in the (*x*, *z*)

and (y, z) planes. The mine's top and bottom positions were input into a MATLAB generated grid, similar to the ones within the pool. The first point to impact the water was always plotted first. This facilitated tracking of the initial entry point throughout the water column. The cameras were not time synchronized; thus, the first recorded position corresponded to when the full length of the mine was in view.

B. Source of Errors

There were several sources of error that hindered the determination of the mine's exact position within the water column. Locations above or below the camera's focal point were subjected to parallax distortion. Placing the cameras as far back as possible, while still being able to resolve the individual grid squares, minimized this error. Second, the background grids were located behind the mine's trajectory plane. This resulted in the mine appearing larger than normal. This error was minimized by not allowing the plotted points to exceed the particular mine's length. Third, an object injected into the water will generate an air cavity. This air cavity can greatly affect the initial motion, particularly at very high speeds (hydro ballistics). The air cavity effect was deemed to be minimal due to the low inject velocities used.

C. Data Analysis

The 3-D data provided by each camera was first used to produce raw two 2-D plots of the mine's trajectory. Next, 2-D data from both cameras was then fused to produce a 3-D history. This 3-D history was then made non-dimensional in order to generalize the results. The non-dimensional data was used to generate impact scatter plots and was also used in multiple linear regression calculations.

6. EXPERIMENTAL RESULTS

A. Trajectory Patterns

After analyzing the 3-D data set, seven trajectory patterns were found. The plots on the (y, z) plane were chosen for trajectory analysis, as this plane was parallel to the direction of the mine drop. The generalized trajectory patterns are described in Table 3, and Figures 7-10. The water phase trajectory a mine experiences ultimately determines the impact orientation. In MIDEX, the categorizing of trajectories into general patterns served two purposes. Observed trajectories were found to be most sensitive to χ-value, drop angle and L/D ratio. As COM distance (χ-value) increased from GC the mine tended to follow a straight pattern. As COM was moved closer to the GC (decreasing χ-value) the mine's trajectory tended towards being more parallel with the pool's bottom. At steep drop angles, the mine experienced little lateral movement and tended towards a straight pattern. Additionally, as L/D ratio decreased more complex trajectory patterns developed. This included significant oscillation about the vertical axis and increased lateral movement.

Table 3. Description of relative coordinate based trajectory patterns.

Trajectory Pattern	Description
Straight (or Slant)	Little angular change, Nearly parallel to z-axis, ψ_2 near ($90^o \pm 15^o$)
Spiral	Oscillating (no rotation)
Flip	Only once as $\chi^* < 0$
Flat	ψ_2 near 0^o (no oscillation)
Seesaw	ψ_2 near 0^o (oscillation)
Combination	Several of the above patterns

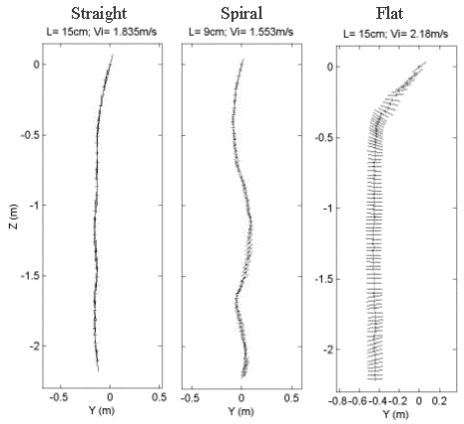

Figure 7. Trajectory patterns.

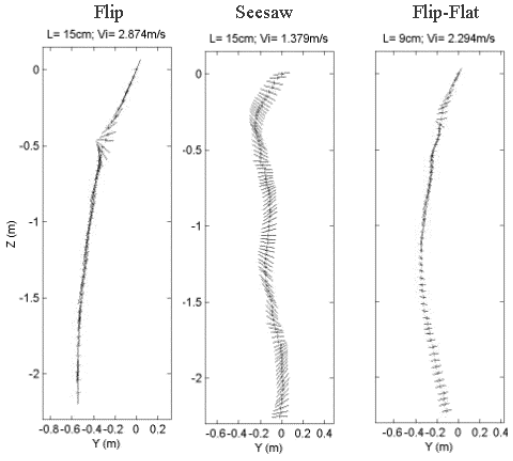

Figure 8. Trajectory patterns.

	COM Position: 2		
Mine Length:	15	12	9
Drop Angle: 15°	Straight	Straight	Straight-Slant
	Slant-Straight	Spiral	Spiral
	Slant-Straight	Slant-Straight	Slant-Straight
	Slant-Straight	Slant-Straight	Spiral
Drop Angle: 30°	Slant-Straight	Slant	Spiral
	Straight	Spiral	Spiral
	Slant-Straight	Straight	Spiral
	Slant-Straight	Slant-Straight	Spiral
	Slant-Straight	Slant-Straight	Spiral
Drop Angle: 45°	Slant-Straight	Spiral	Spiral
	Slant	Spiral	Spiral
	Straight-Spiral	Straight-Spiral	Spiral
	Straight	Straight	Spiral
	Slant	Slant-Straight	Slant-Spiral
Drop Angle: 60°	Straight	Straight-Slant	Spiral
	Straight	Straight	Spiral
	Straight	Straight	Spiral
	Straight	Straight-Spiral	Straight-Spiral
	Straight	Straight	Spiral
Drop Angle: 75 °	Straight	Straight	Spiral
	Straight	Straight-Spiral	Slant
	Straight	Straight	Spiral
	Straight	Straight-Spiral	Straight-Spiral
	Straight	Straight-Spiral	Straight-Spiral

Figure 9. Trajectory patterns for $\chi = \chi_2$.

	COM Position: -2		
Mine Length:	15	12	9
Drop Angle: 30°	Flip-Straight	Flip-Slant	Flip-Straight-Spiral
	Flip-Straight	Flip-Straight	Flip-Straight-Spiral-Flip
Drop Angle: 45°	Flip-Straight	Flip-Straight-Spiral	Flip-Straight
	Flip-Straight	Flip-Straight	Flip-Straight-Spiral
	COM Position: -1		
Drop Angle: 30°	Flip-Straight	Flip-Slant	Straight-Flip-Seesaw
	Flip-Slant	Flip-Straight	Flip-Straight-Spiral
Drop Angle: 45°	Flip-Spiral-Slant	Flip-Slant	Flip-Spiral
	Flip-Slant	Flip-Slant	Flip-Spiral
Drop Angle: 60°	Flip-Straight	Flip-Straight	Flip-Spiral-Seesaw
	Straight-Flip	Slant-Flip-Slant	Flip-Spiral

Figure 10. Trajectory patterns for negative COM position (χ_{-1}, χ_{-2}). Here, COM is above GC when the cylinder enters the surface).

B. Impact Attitude

The angle, $\psi_2 + \pi/2$, is the impact attitude at the bottom of the water column. The mine burial is largely determined from the impact attitude of the mine. Mines whose impact attitudes are perpendicular ($\psi_2 = 90^o$) to the sediment interface will experience the largest degree of impact burial (Taber 1999). It is therefore important to analyze the relationship between impact attitude and the controlled parameters, drop angle, V_{in}, L/D, and χ. The experiment shows that both L/D and V_{in} had little influence on impact attitude. The drop angle and χ, however, were the largest determinants of impact attitude.

From Figure 11 it is apparent that there are several peaks centered near 90°, 140°, and 180°. Further analysis reveals that these peaks correspond to the COM positions 0, 1 and 2 (corresponding to χ_0, χ_1, χ_2), respectively. COM positions -1 and -2 (corresponding to χ_{-1}, χ_{-2}) followed the same trend as their positive counterparts.

Although drop angle was not the most influential parameter, variations did induce changes in impact orientation. As drop angle increased, the likelihood of any lateral movement decreased. This allowed for impact angles that were more vertically orientated. This is primarily due to the fact that the vertical components of velocity were greater than those at shallow angles. Thus, the time to bottom and time for trajectory alteration was less.

C. Mine Tumbling Not Observed

The current Navy's mine impact burial model (IMPACT25/28) was developed by the Coastal System Station (Arnone and Bowen 1980; Satkowiak 1987); subsequent upgraded by the New Zealand Defense Establishment (Hurst 1992) and the Naval Research Laboratory (NRL). Some of the major input parameters to the model are environment (sedimentation, shear strength, water depth), mine characteristics (shape, center of mass, weight, and mine deployment parameters), deployment platform (ship, aircraft, submarine), speed of platform, angle of mine upon entering water, rotational velocity at time of deployment and others. The theoretical base of IMPACT25 is the momentum equations (2a)-(2c). The model assumes that COM coincides with GC ($\chi = 0$). Chu et al. (2001) reported the discrepancy between observed and model predicted (by IMPACT25/28) mine burial depth from a mine impact burial experiment performed near the Monterey beach, California in May 2000. The model describes two trajectory patterns (Figure 12): (a) without any orientation change, (b) with a constant tumbling. For the second pattern, user should input the tumbling rate (Chu et al. 1998; 2000a,b). In MIDEX, mine tumbling was never observed even for $\chi = 0$ (Figure 13).

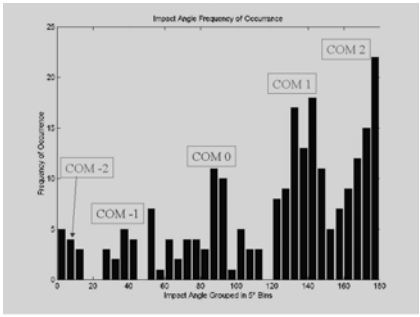

Figure 11. Relationship between COM position and impact attitude.

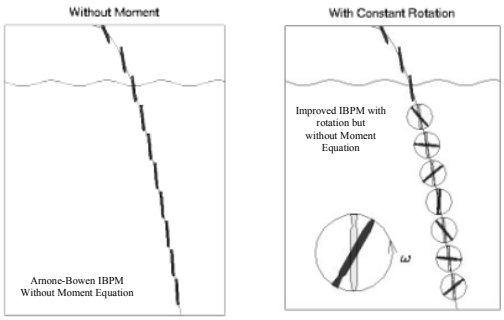

Figure 12. Two trajectory patterns predicted using the Navy's Mine Impact Burial Model (IMPACT25/28): (a) no tumbling, and (b) constant tumbling. The model was established based only on the momentum equations (2a)-(2c).

	COM Position: 0		
Mine Length:	15	12	9
Drop Angle: 15°	Seesaw	Flat	Flat-Seesaw
	Seasaw	Seesaw	Seesaw
	Seasaw	Seesaw	Flat-Seesaw
	Flat	Spiral-Seesaw	Spiral-Seesaw
Drop Angle: 30°	Seesaw	Flat	Spiral-Seesaw
	Flat	Flat-Spiral	Flat-Spiral
	Flat-Spiral	Flat-Spiral	Flat-Spiral
	Flat	Flat-Spiral	Flat-Spiral
	Slant-Seesaw	Spiral-Flat-Seesaw	Flat
Drop Angle: 45°	Seesaw	Flat-Spiral	Spiral-Seesaw
	Flat-Spiral	Straight-Flat	Straight-Flat
	Straight	Straight-Flat	Straight-Flat-Spiral
	Straight-Flat-Spiral	Seesaw	Seesaw
Drop Angle: 60°	Spiral-Seesaw	Straight-Seesaw	Straight-Flat
	Straight-Spiral-Seesaw	Straight-Spiral-Seesaw	Straight-Flat
	Straight-Spiral-Seesaw	Straight-Flat-Spiral	Straight-Seesaw
	Slant	Straight-Flat	Straight-Spiral-Flat
	Straight-Flat-Spiral	Straight	Straight-Seesaw-Spiral
	Straight-Spiral-Seesaw	Straight-Spiral-Seesaw	Straight-Seesaw
Drop Angle: 75 °	Straight-Seesaw	Straight-Flat	Straight-Spiral-Seesaw
	Straight-Spiral-Seesaw	Straight	Straight-Flat-Spiral

Figure 13. Trajectory patterns for the COM-0 position (i.e., COM coincidence with GC).

7. STATISTICAL PREDICTION MODEL

Multivariate linear regression model was established from the MIDEX data (712 drops) to establish relationships between the input non-dimensional parameters; ψ_2^{in}, L/D, V_{in}, and χ, and the output variables (temporally varying) such as position (x_{m}, y_{m}, z_{m}), velocity (u, v, w) and attitude ψ_2 at time t. Let Y represent the output variables. The regression equation is given by

$$Y(t) = \beta_0(t) + \beta_1(t)\psi_2^{in} + \beta_2(t)L/D + \beta_3(t)V_{in} + \beta_4(t)\chi. \qquad (9)$$

Figure 14 shows the temporally varying regression coefficients for u, v, w, and ψ_2. For the mine's attitude (ψ_2) the coefficient $\beta_4(t)$ is much larger than the other coefficients, which indicates that the mine's orientation (versus the vertical direction) is mainly determined by the location of COM.

To show the dependence of impact of mine on the bottom (i.e., horizontal location relative to the mine's surface entry point, orientation, velocity), the multivariate regression between the input non-dimensional parameters; ψ_2^{in}, L/D, V_{in}, and χ, and the final state (i.e., impact on the bottom) variables such as the horizontal position of COM (x_{m}, y_{m}), the velocity of COM (u, v, w) and the attitude ψ_2. Let Z represent the output variables. The regression equation is given by

$$Z = \alpha_0 + \alpha_1\psi_2^{in} + \alpha_2 L/D + \alpha_3 V_{in} + \alpha_4\chi, \qquad (10)$$

with the regression coefficients ($\alpha_0, \alpha_1, \alpha_2, \alpha_3, \alpha_4$) for the output parameters given by Table 4.

Table 4. Regression coefficients of Eq.(10).

	x_{m}	y_{m}	ψ_2	u	v	w
α_0	-0.07	-0.05	103.0	0.0040	-0.014	-0.948
α_1	0.119	-0.83	-13.4	-0.008	-0.0106	-0.108
α_2	-0.47	-0.08	-0.501	-0.110	0.0005	0.0295
α_3	0.037	0.062	1.045	0.0025	0.0011	-0.221
α_4	0.237	0.433	472.0	-0.009	0.0537	-1.25

8. CONCLUSIONS

(1) Moment of a falling mine in water column is a highly nonlinear process, which should be described by both the momentum and moment of momentum equations. If the moment of momentum equations are absent, the motion of falling mine cannot be completely simulated. The new mine impact burial prediction model should include the moment of momentum equations.

(2) Six different trajectory patterns (straight, spiral, flip, flat, seesaw, combination) were detected from MIDEX. No tumbling of mine was observed. The flip of mine occurs only once for negative χ-values (i.e., COM is above GC as the mine enters the water surface). The flat pattern occurs usually for χ = 0 (i.e., COM coincides with GC). The transition between patterns depends on the initial conditions (drop angle ψ_2^{in} and initial velocity V_{in}) and the internal structure of mine (such as L/D ratio, χ-value, etc.). The dynamics of trajectory pattern formation and transition is very complicated. It involves stability, nonlinear dynamics, and fluid-body interaction.

(3) MIDEX shows that both L/D and V_{in} had little influence on mine's impact attitude on the bottom. The drop angle ψ_2^{in} and χ, however, were the determinants of impact attitude. For χ =0, the mine was almost parallel to the bottom. For χ_{-2} and χ_2 cases, the mine is almost vertical to the bottom.

(4) MIDEX provided nondimensional data of position (x_{m}, y_{m}, z_{m}), velocity (u, v, w) and attitude ψ_2 for each input including data ψ_2^{in}, L/D ratio, V_{in}, and χ. The data can be used for model development and validation.

(5) The observed trajectories were far more complex than those theorized by using only the momentum equations. Simply assigning a rotation rate into the model will not simulate the movement of falling mine in the water column. At a minimum, updates to the IMPACT 25 model

should include the more realistic moment of momentum equations.

(6) Further research on mine hydrodynamics is needed. The research needs to expand beyond the simple cylindrical shaped mine to those that are irregularly shaped (Rockan and Manta types). Additionally, the utilization of scaled down versions should be explored. A smaller mine that can be modeled as accurately as its real counterpart will save time, money and will require less logistical support.

ACKNOWLEDGMENT

This work was supported by the Office of Naval Research Marine Geology Program (N0001401WR20218) and the Naval Oceanographic Office (N6230600PO00005).

REFERENCES

Arnone, R. A., and Bowen, Prediction Model of the Time History Penetration of a Cylinder through the Air-Water-Sediment Phases. NCSC letter report T34, Naval Coastal Systems Center, Panama City, FL, 1980.

Boorda, J. M., "Mine Countermeasures - An Integral Part of our Strategy and our Forces." Federation of American Scientists. (http://www.fas.org/man/dod-101/sys/ship/weaps/docs/cnopaper.htm)

Chu, P.C., E. Gottshall, and T.E. Halwachs, 1998: Environmental Effects on Naval Warfare Simulations. Institute of Joint Warfare Analysis, Naval Postgraduate School, Technical Report, NPS-IJWA-98-006, 33p.

Chu, P.C., V.I. Taber, and S.D. Haeger, 2000a: A Mine Impact Burial Model Sensitivity Study. Institute of Joint Warfare Analysis, Naval Postgraduate School, Technical Report, NPS-IJWA-00-003, 48p.

Chu, P.C., V.I. Taber, and S.D. Haeger, 2000b: Environmental Sensitivity Study on Mine Impact Burial Prediction Model. Proceedings on the Fourth International Symposium on Technology and the Mine Problem, 10 pp.

Chu, P.C., T.B. Smith, and S.D. Haeger, 2001: Mine burial impact prediction experiment. Institute of Joint Warfare Analysis, Naval Postgraduate School, Technical Report, NPS-IJWA-01-007, 161p.

Department of the Navy. U.S. Naval Mine Warfare Plan Fourth Edition, Programs for the Millennium. Washington, D.C., January 2000.

Fischer, Ben B. At Cold War's End: US Intelligence on the Soviet Union and Eastern Europe, 1989-1991. Springfield: National Technical Information Service, 1999.

Hurst, R.B. Mine Impact Burial Prediction Model - Technical Description of Recent Changes and Developments. Defense Scientific Establishment, Auckland, New Zealand, Report 149.

Lehr, S.E., Mine Warfare: To Enable Maneuver, Amphibious Warfare Conference, 26 April 2000. (http:// www.exwar.org/awcfinal/6th/n852mines.ppt)

Lott, D.F., K. Williams, and D. Jackson, Mine Burial in Carbonate Sediments. Proc. of the Technology and Mine Problem Symposium, November 1996, Naval Postgraduate School.

Rhodes, J.E., G. Holder, Concept for Future Naval Mine Countermeasures in Littoral Power Projection, 1 May 1998. (http:// 192.156.75.102/mcm.htm)

Satkowiak, L. J., User's Guide for the Modified Impact Burial Prediction Model. NCSC TN 884-87. Naval Coastal Systems Center, Panama City, Fl, 1987.

Smith, T., Mine Burial Impact Prediction Experiment. Master Thesis, Naval Postgraduate School, Monterey, CA, 2000.

Taber, V., Environmental Sensitivity Study on Mine Impact Burial Prediction Model. Master Thesis, Naval Postgraduate School, Monterey, CA, 1999.

Peter C. Chu (PhD, 85') is a professor of oceanography, joint warfare analysis, and modeling and virtue environment simulation (MOVES) at the Naval Postgraduate School, Monterey, CA 93943.
Chenwu Fan (MA, 82')Is an oceanographer at the Naval Postgraduate School, Monterey, CA 93943.
Peter Fleischer (Ph.D, 70') is an oceanographer at the Naval Oceanographic Office, Stennis Space Center, MS 39529.
Anthony F. Gilles (MA, 01) is a Navy Lieutenant Commander who obtained MA degree in Meteorology and Oceanography at the Naval Postgraduate School in September 2001.